

The lncRNA *PCAT29* Inhibits Oncogenic Phenotypes in Prostate Cancer

Rohit Malik^{1,2}, Lalit Patel^{1,2}, John R. Prensner^{1,2}, Yang Shi^{1,3}, Matthew K. Iyer^{1,2}, Shruthi Subramanian¹, Alexander Carley¹, Yashar S. Niknafs^{1,2}, Anirban Sahu^{1,2}, Sumin Han^{1,4}, Teng Ma^{1,4}, Meilan Liu⁴, Irfan A. Asangani^{1,2}, Xiaojun Jing^{1,2}, Xuhong Cao^{1,2}, Saravana M. Dhanasekaran^{1,2}, Dan R. Robinson^{1,2}, Felix Y. Feng^{1,4,5}, and Arul M. Chinnaiyan^{1,2,5,6}

Abstract

Long noncoding RNAs (lncRNA) have recently been associated with the development and progression of a variety of human cancers. However, to date, the interplay between known oncogenic or tumor-suppressive events and lncRNAs has not been well described. Here, the novel lncRNA, prostate cancer-associated transcript 29 (*PCAT29*), is characterized along with its relationship to the androgen receptor. *PCAT29* is suppressed by DHT and upregulated upon castration therapy in a prostate cancer xenograft model. *PCAT29* knockdown significantly increased proliferation and migration of prostate cancer cells, whereas *PCAT29* overexpression conferred the opposite effect and suppressed growth and metastases of prostate tumors in chick chorioallantoic membrane assays. Finally, in prostate cancer patient specimens, low *PCAT29* expression correlated with poor prognostic outcomes. Taken together, these data expose *PCAT29* as an androgen-regulated tumor suppressor in prostate cancer.

Implications: This study identifies *PCAT29* as the first androgen receptor-repressed lncRNA that functions as a tumor suppressor and that its loss may identify a subset of patients at higher risk for disease recurrence.

Visual Overview: <http://mcr.aacrjournals.org/content/early/2014/07/31/1541-7786.MCR-14-0257/F1.large.jpg>.

Mol Cancer Res; 12(8); 1081–7. ©2014 AACR.

Introduction

Recently, data from the ENCODE project have revealed that the majority of the transcriptome is composed of noncoding RNAs (1). While the classification of these noncoding RNAs is still in development, long noncoding RNAs (lncRNA) are of particular interest, given the similar features they share with protein-coding genes as well as recent evidence of their roles in cancer biology (2, 3). LncRNAs are polyadenylated RNA species that are more

than 200 bp in length, transcribed by RNA polymerase II, and associated with common epigenetic signatures such as of histone 3 lysine 4 trimethylation (H3K4me3) at the transcriptional start site (TSS) and histone 3 lysine 36 trimethylation (H3K36me3) in the gene body (4). Several lncRNAs have been shown to play a role in biologic processes such as X-chromosomal inactivation, pluripotency (5), and gene regulation (6). Recently, several lncRNAs have been implicated in cancer initiation and progression (3, 7). Apart from their role in tumor initiation and progression, lncRNAs have been shown to be promising biomarkers. In prostate cancer, PCA3 is a well-studied prostate cancer biomarker that is now available for clinical use as a urine biomarker assay for diagnosis of prostate cancer (8, 9).

Despite their involvement in various cellular processes, the majority of lncRNAs are uncharacterized, and their role in cancer initiation and progression remains unclear. Using transcriptome sequencing, our group recently identified more than 100 lncRNAs, named prostate cancer-associated transcripts (*PCATs*), which are differentially expressed or have outlier profiles in prostate cancer versus normal tissue (3). Here we find that one of these novel lncRNAs, *PCAT29*, exhibits cancer-suppressive phenotypes, including inhibition of cell proliferation, migration, tumor growth, and metastases. In accordance with this, *PCAT29* is repressed by androgen signaling, and low *PCAT29* expression associates with worse clinical outcomes.

¹Michigan Center for Translational Pathology, University of Michigan, Ann Arbor, Michigan. ²Department of Pathology, University of Michigan, Ann Arbor, Michigan. ³Department of Biostatistics, University of Michigan, Ann Arbor, Michigan. ⁴Department of Radiation Oncology, University of Michigan, Ann Arbor, Michigan. ⁵Comprehensive Cancer Center, University of Michigan, Ann Arbor, Michigan. ⁶Howard Hughes Medical Institute, University of Michigan, Ann Arbor, Michigan.

Note: Supplementary data for this article are available at Molecular Cancer Research Online (<http://mcr.aacrjournals.org/>).

F.Y. Feng and A.M. Chinnaiyan share senior authorship of this article.

Corresponding Authors: Arul M. Chinnaiyan, Comprehensive Cancer Center, University of Michigan Medical School, 1400 E. Medical Center Dr. 5316 CCGC 5940, Ann Arbor, MI 48109. Phone: 734-615-4062; Fax: 734-615-4055; E-mail: arul@med.umich.edu; and Felix Y. Feng, Department of Radiation Oncology, University of Michigan Medical Center, 1500 East Medical Center Drive, UHB2C490-SPC5010, Ann Arbor, MI 48109. Phone: 734-936-4302; Fax: 734-763-7371; E-mail: ffeng@med.umich.edu

doi: 10.1158/1541-7786.MCR-14-0257

©2014 American Association for Cancer Research.

Materials and Methods

Cell lines and reagents

Prostate cancer cells were cultured as follows: VCaP cells in DMEM with GlutaMAX (Invitrogen) and LNCaP and DU145 cells in RPMI-1640 (Invitrogen) in a 5% CO₂ cell culture incubator. All the media were supplemented with 10% FBS (Invitrogen) and 1% penicillin–streptomycin (Invitrogen). All cell lines were purchased from ATCC and were authenticated.

For stable knockdown of *PCAT29*, LNCaP and VCaP cells were transfected with lentiviral constructs encoding 2 different *PCAT29* shRNAs or nontargeting shRNAs in the presence of polybrene (8 µg/mL; Supplementary Table S1A). After 48 hours, transduced cells were grown in culture media containing 3 to 5 µg/mL puromycin. For *PCAT29* overexpression, 2 isoforms of *PCAT29* were generated by subcloning the PCR product into the *CPOI* sites of the pCDH-CMV vector (System Biosciences). Five hundred base pairs of the genomic region was attached at the 5' end of each isoform. Lentiviral particles were made and DU145 cells were transduced as described above.

Gene expression by quantitative PCR

Total RNA was isolated using TRIzol (Invitrogen) and an RNeasy kit (Qiagen) according to manufacturers' instruction. Total RNA was reverse transcribed into cDNA using SuperScript III and random primers (Invitrogen). Quantitative PCR (qPCR) was performed using SYBR Green Master Mix (Applied Biosystems) on an Applied Biosystems 7900HT Real-Time System. The relative quantity of the target gene was computed for each sample using the $\Delta\Delta C_t$ method by comparing mean C_t of the gene to the mean C_t of the housekeeping gene *GAPDH*. All the primers were obtained from Integrated DNA Technologies (IDT). Sequences of all the primers used are listed in Supplementary Table S1B.

Rapid amplification of cDNA ends

5' and 3' RACE was performed using the GeneRacer RLM-RACE kit (Invitrogen) following manufacturer's instruction. RACE PCR products were separated on a 1% agarose gel. Individual bands were gel purified, cloned in pcr4-TOPO vector, and sequenced using M13 primers.

Expression of *PCAT29* after castration in prostate tumor xenograft model

Five-week-old male nude athymic BALB/c *nu/nu* mice (Charles River Laboratory) were used for xenograft studies. LNCaP cells were resuspended in 100 µL of PBS with 20% Matrigel (BD Biosciences) and implanted subcutaneously into the left flank regions of the mice. Mice were castrated and euthanized 5 days after castration. RNA was extracted from the xenografts and expression of *PCAT29* and *FKBP5* was measured. All experimental procedures involving mice were approved by the University Committee on Use and Care of Animals at the University of Michigan (Ann Arbor, MI) and conform to their relevant regulatory standards.

Chromatin immunoprecipitation

Chromatin immunoprecipitation (ChIP) was performed with polyclonal androgen receptor antibody (Millipore PG21) using HiCell ChIP kit (Diagenode) following manufacturer's instruction. Briefly, cells were treated with 10 µmol/L MDV3100 or 10 µmol/L bicalutamide 16 hours before the treatment with 10 nmol/L DHT for 12 hours. Approximately 1 million cells were cross-linked per antibody with 1% formaldehyde. Chromatin was sonicated to an average length of 500 bp and centrifuged to remove debris. Magnetic protein-G beads were coated with 6 µg of antibody and incubated with chromatin overnight at 4°C. Protein–chromatin–antibody complexes were washed thrice and cross-linking was reversed. ChIP products were cleaned using IPure kit (Diagenode). Eluted DNA was quantified by RT-PCR using primers described in Supplementary Table S1B.

Cell proliferation and migration assay

LNCaP and DU145 cells stably expressing *PCAT29* shRNA-1 and 2 or *PCAT29* isoform 1 and 2 were seeded in 24-well plates. Cells were trypsinized and counted by using Coulter Counter (Beckman Coulter) at the indicated time points in triplicate. For migration assays, approximately 1×10^5 cells were seeded in the upper chamber of a Boyden chamber. About 500 µL of complete medium (10% FBS) was added to the lower chamber as a chemoattractant. Forty-eight hours after seeding, cells on the upper surface were removed using a cotton swab. Inserts were fixed with 3.7% formaldehyde and migrated cells on the lower surface of the membrane were stained with crystal violet. The inserts were treated with 10% acetic acid, and absorbance was measured at 560 nm.

Gene expression microarray

Expression profiling of VCaP and LNCaP cells after *PCAT29* knockdown was performed using the Agilent Whole Human Genome Oligo Microarray as described (7). GEO accession number: GSE58397.

Chicken chorioallantoic membrane assay

22RV1 cells were transduced with empty vector (pcDH) or *PCAT29*-isoform-1. A total of 10^6 cells were inoculated on the chicken chorioallantoic membrane (CAM) assay as described previously (10). For tumor growth and metastasis, the eggs were incubated for 18 days in total, after which the extra-embryonic tumor were exercised and weighed, and the embryonic livers were harvested and analyzed for the presence of tumor cells by quantitative human Alu-specific PCR. Quantification of human cells in the extracted DNA was performed as described (11). Fluorogenic TaqMan qPCR probes were applied as above and DNA copy numbers were quantified.

Kaplan–Meier analysis of *PCAT29*

For outcomes analysis, *PCAT29* expression was determined on a cohort of 51 radical prostatectomy specimens from patients with prostate cancer at the University of

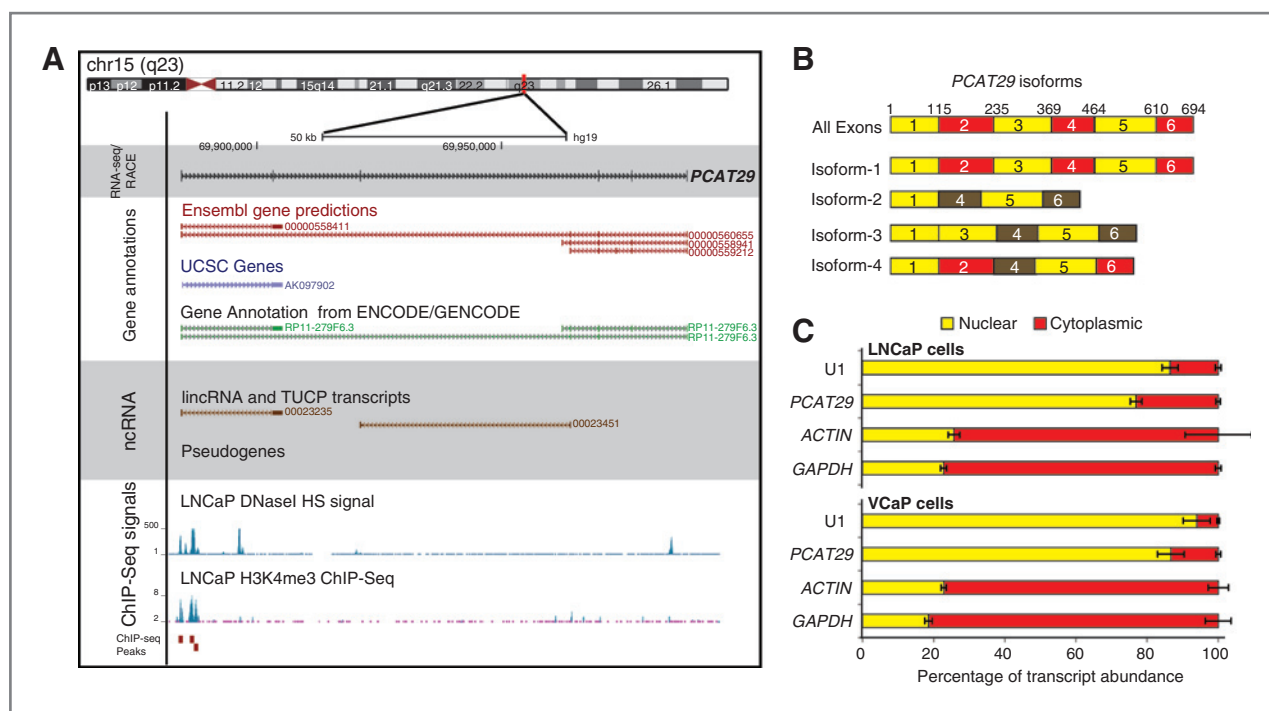


Figure 1. Characterization of *PCAT29*. A, genome browser representation of *PCAT29*. Current gene annotations from Ensembl, ENCODE, UCSC genes and lincRNA databases are shown. ChIP-Seq data for H3K4me3 and DNaseI HS signal in LNCaP cells obtained from ENCODE. B, schematic representation of *PCAT29* isoforms as determined by RACE analysis. C, nuclear and cytoplasmic distribution of various noncoding and protein-coding transcripts in LNCaP and VCaP cells. Error bar, \pm SEM.

Michigan with long-term biochemical recurrence outcomes. Biochemical recurrence was defined by an increase of PSA of 0.2 ng/mL over the PSA nadir following prostatectomy. *PCAT29* expression was determined by a SYBR-Green qPCR assay using the average of *GAPDH* + *HMBS* for data normalization using the $\Delta\Delta C_t$ method. Expression data were transformed using a z -score and patients were defined as high (top 33% of patients) or low (bottom 66% of patients) for *PCAT29* expression. Kaplan–Meier curves for biochemical recurrence-free survival were generated for *PCAT29*-high and *PCAT29*-low patients using the GraphPad Prism program. Statistical significance was determined with a log-rank test.

Results

PCAT29 is a novel long nuclear noncoding RNA

Using RNA-Seq data from prostate cancer tissues, we previously identified 121 lincRNAs, named PCATs, which demonstrate differential expression or outlier profiles in prostate cancer compared with normal tissue (3). Here we characterize and functionally investigate one of the top outlier lincRNAs, *PCAT29* (Ensembl ID ENSG00000259641). Using the predicted transcript structures, we designed exon spanning primers and performed rapid amplification of cDNA ends (RACE) to determine the full exon structure. As shown in a genome browser view, *PCAT29* is a 694-bp polyadenylated transcript present on chr15(q23), and the *PCAT29* gene spans over a 10-kb stretch (Fig. 1A; Supple-

mentary Fig. S1A). *PCAT29* is composed of 6 exons that are alternatively spliced to produce multiple isoforms (Fig. 1B). To further characterize *PCAT29*, we interrogated recently published ENCODE data for H3K4 trimethylation (H3K4me3) and DNaseI hypersensitive sites (DNaseH), marks that predicts for open chromatin state and are commonly found near or at the TSSs, generated in the prostate cancer cell line LNCaP (4). We found several DNaseH and H3K4 trimethylation peaks at the TSS of *PCAT29*, suggesting that *PCAT29* is an actively transcribed gene (Fig. 1A).

To confirm that *PCAT29* is indeed a noncoding RNA, we assessed the protein-coding potential of *PCAT29* using the coding potential calculator (CPC) algorithm, which discriminates coding genes (positive score) from noncoding transcripts (negative score; ref. 12). *PCAT29* had a CPC score of -0.8921 , whereas protein-coding genes such as *TP53* and β -actin scored $+8.25$ and $+3.70$, respectively (Supplementary Fig. S1B). Consistent with this finding, we found that in both LNCaP and VCaP cells, expression of *PCAT29* was limited to nucleus, whereas other protein-coding mRNAs, such as *GAPDH* and β -actin, were expressed in cytoplasm (Fig. 1C). We then verified the expression of *PCAT29* in various prostate cancer cell lines (LNCaP, VCaP, 22RV1, DU145, PC3) and immortalized or primary prostate epithelial cells (RPWE and PrEC). *PCAT29* expression was highest in androgen receptor-dependent cell lines such as LNCaP, VCaP, and 22RV1 (Supplementary Fig. S1C).

Next, we assessed the expression of *PCAT29* in various tissues using transcriptome sequencing data. *PCAT29* expression, although not limited to prostate, was enriched in prostate samples compared with other tissues (Supplementary Fig. S1D).

Androgen receptor binds to the *PCAT29* promoter and regulates *PCAT29* expression

We next examined the effect of androgen receptor signaling on *PCAT29* in LNCaP cells stimulated with 10 nmol/L DHT. As shown in Fig. 2A, *PCAT29* expression was suppressed upon stimulation with DHT in a time-dependent fashion both in LNCaP and VCaP cells. In contrast, expression of canonical androgen receptor target genes, such as *FKBP5* and *KLK3*, was increased upon stimulation (Supplementary Fig. S2A). To examine whether the suppression of *PCAT29* was androgen receptor-specific, LNCaP cells

were pretreated with the androgen receptor antagonists MDV3100 or bicalutamide before treatment with DHT. As expected, DHT stimulation suppressed the expression of *PCAT29*, and pretreatment with MDV3100 or bicalutamide rescued this suppression. Similarly, expression of *PCAT29* in LNCaP cells grown in charcoal-stripped media as well as in an androgen receptor-independent variant of LNCaP cells (C42) was higher than in cells grown in serum-containing media and LNCaP cells, respectively (Supplementary Fig. S2B and S2C). We next investigated whether androgen receptor suppresses the expression of *PCAT29* *in vivo*. LNCaP xenografts were established in mice followed by physical castration to ablate androgen receptor signaling. As expected, 5 days of castration led to significant increase in the expression of *PCAT29* in tumors (Fig. 2C). In contrast, expression of *FKBP5* was reduced in tumors from castrated mice. Taken together, our results suggest that stimulation

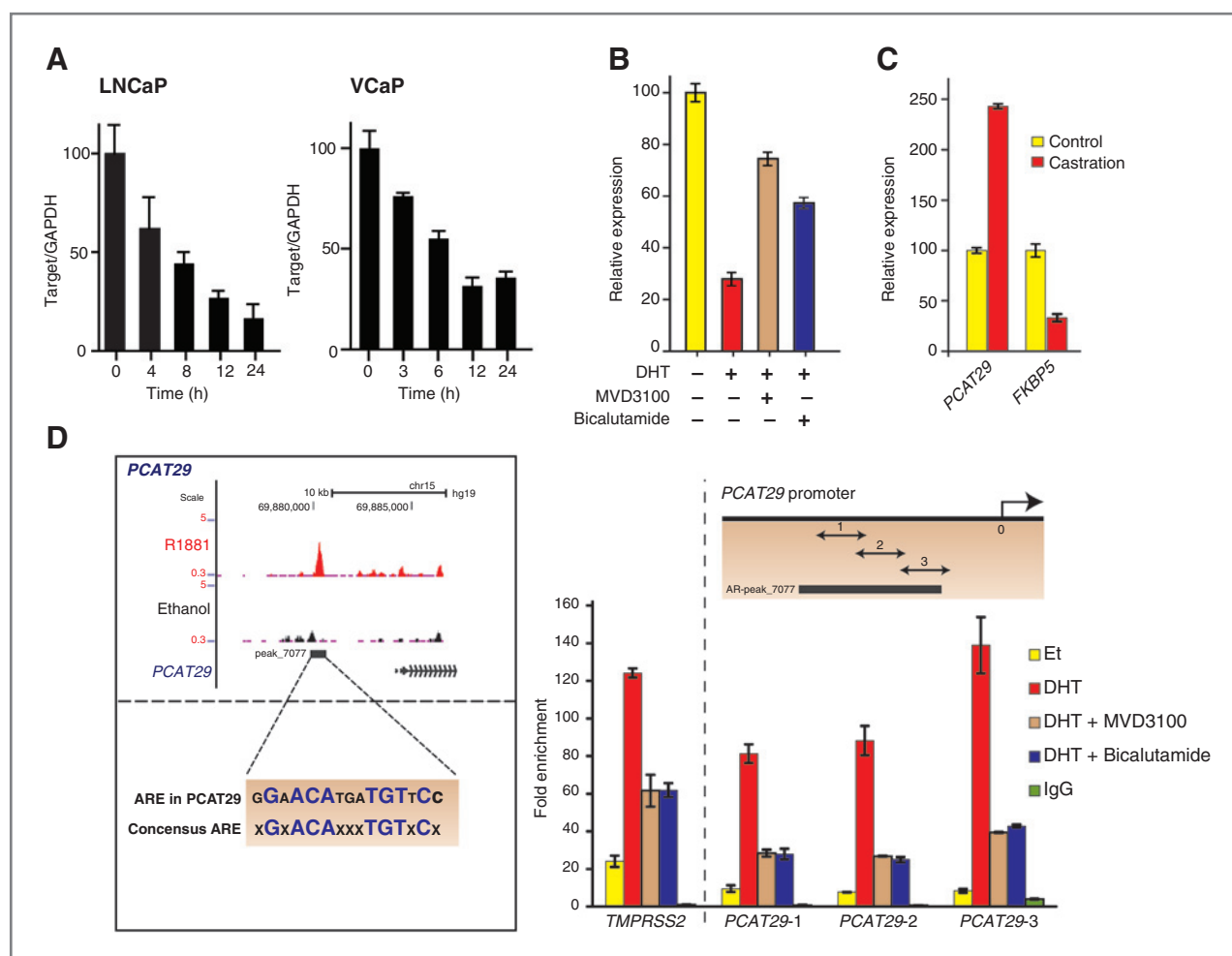


Figure 2. Androgen receptor binds to the promoter of *PCAT29* and suppresses its expression. A, expression of *PCAT29* in LNCaP and VCaP cells treated with 10 nmol/L DHT for indicated time points. B, expression of *PCAT29* in LNCaP cells treated with 10 nmol/L DHT in the presence or absence of 10 μ mol/L MDV3100 or bicalutamide. C, expression of *PCAT29* and *FKBP5* in LNCaP xenografts obtained from control mice and mice that were physically castrated for 5 days. D, genome browser representation of androgen receptor (AR) binding on the promoter of *PCAT29* before and after stimulation with 1 nmol/L R1881. Consensus androgen-responsive elements (ARE) and ARE present in the *PCAT29* promoter are shown. Inset, ChIP-PCR to confirm AR occupancy on *TMPRSS2* and *PCAT29* gene promoter. The y-axis represents AR ChIP enrichment in VCaP cells treated with 10 nmol/L DHT normalized to ethanol (Ethl)-treated cells. Bars, SEM.

of androgen receptor leads to suppression of *PCAT29* expression.

To further study the association of *PCAT29* expression with androgen signaling, we interrogated published ChIP-Seq data (13) and found androgen receptor-binding sites in the promoter region of *PCAT29* (Fig. 2D). These peaks were similar to those observed in other known androgen receptor-regulated genes (Supplementary Fig. S2D). Upon closer inspection, we found a canonical androgen receptor-binding site near the *PCAT29* TSS in a putative enhancer region bound by androgen receptor (Fig. 2D). We confirmed our ChIP-Seq data by performing ChIP for androgen receptor followed by PCR for the *PCAT29* promoter. As shown in Fig. 2D, stimulation of VCaP cells with DHT led to an increase in association of androgen receptor with the *PCAT29* promoter. This association was reduced in cells pretreated with bicalutamide and MDV3100. Taken together, our data suggest that androgen receptor can directly bind to the promoter of *PCAT29* and leads to the suppression of gene expression.

PCAT29* regulates oncogenic phenotypes *in vitro* and *in vivo

The androgen receptor drives oncogenesis in treatment-naïve prostate cancer as well as disease progression in castration-resistant prostate cancers. Because androgen receptor binds to the *PCAT29* promoter and regulates gene expression, we investigated the functional role of *PCAT29*. Two independent shRNAs were designed to knockdown the expression of *PCAT29* in cells (Supplementary Fig. S3A and S3B). VCaP and LNCaP cells were transfected with *PCAT29* shRNAs following analysis using gene expression microarray. We found GO concepts enriched for cell cycle, proliferation, and migration-related genes, suggesting a role of *PCAT29* in proliferation and migration (Supplementary Fig. S3D–S3G). Next, we defined a signature of genes positively and negatively correlated with *PCAT29* expression from prostate cancer samples as described before (7). We checked the overlap of these genes with the top 1500 differentially expressed genes in *PCAT29* knockdown samples of VCaP and LNCaP cells. As expected, the positively correlated genes show a significant overlap with genes downregulated with knockdown of *PCAT29* and the negatively correlated genes show a significant overlap with genes upregulated by knockdown of *PCAT29* in both VCaP and LNCaP ($P < 0.001$ for all pairwise comparisons of overlapping genes, Supplementary Fig. S4A–S4D). For overlapping genes, we did see enrichment in pathways such as cell cycle, apoptosis, and cell growth (Supplementary Fig. S4A–S4D). Taken together, this analysis suggested a role of *PCAT29* in cell proliferation and migration.

To experimentally validate this observation, cell proliferation was assessed in LNCaP cells transfected with control versus *PCAT29* shRNAs. To our surprise, knockdown of *PCAT29* in LNCaP cells led to an increase in cell proliferation and migration (Fig. 3A). To further validate this observation, we stably overexpressed the 2 most prevalent isoforms of *PCAT29* in DU145 prostate cancer cells using a

lentiviral vector (Supplementary Fig. S3C). Consistent with the previous knockdown studies, overexpression of these 2 isoforms of *PCAT29* in DU145 led to suppression of cell proliferation and migration (Fig. 3B). We next assessed whether similar effects of *PCAT29* could be achieved *in vivo*. 22RV1 prostate cancer cells overexpressing *PCAT29* (isoform-1) were implanted on the CAM of a chicken egg. Compared with control cells, overexpression of *PCAT29* significantly decreased the growth of tumor on the CAM as well as decreased liver metastases (Fig. 3C).

Finally, we measured the expression of *PCAT29* in an independent cohort of 51 radical prostatectomy specimens from patients with prostate cancer with localized disease and clinical follow-up. As shown in Kaplan–Meier analysis (Fig. 3D), patients with lower *PCAT29* expression had significantly higher rates of biochemical recurrence, consistent with our *in vitro* and *in vivo* findings.

Discussion

In this study, we characterize the novel lncRNA *PCAT29*. Our findings demonstrate that *PCAT29* is directly regulated by the androgen receptor, which binds to the promoter of *PCAT29* and suppresses its transcription. *In vitro* studies show that *PCAT29* negatively regulates prostate cancer proliferation and migration, and CAM assays demonstrate that *PCAT29* inhibits tumor growth and metastases. Low expression of *PCAT29* is associated with higher rates of biochemical recurrence, suggesting that *PCAT29* represses oncogenic phenotypes via a tumor-suppressive role.

While previous studies have nominated and characterized lncRNAs that are dysregulated in cancer (3, 14), the majority of characterized lncRNAs, to date, has been associated with oncogenic roles instead of tumor suppressor functions. In fact, there have been only a handful of lncRNAs identified to date that function in repression of cancer phenotypes, and, to our knowledge, none of these are targets downregulated by known oncogenes (14). A recent study identifies a protein-coding gene, *CCN3/NOV*, as a tumor suppressor that is repressed by androgen receptor (15). Thus, our study represents the first identification of an androgen receptor-repressed lncRNA functioning as a tumor suppressor. While further studies will be required to identify the mechanism of *PCAT29* and other tumor suppressor lncRNAs, it is clear that these lncRNAs represent an intriguing area for exploration in cancer biology.

In the context of prostate cancer, androgen-regulated lncRNAs are of fundamental importance, given that all stages of prostate cancer are exquisitely dependent on androgen receptor signaling for growth and survival. Because the majority of clinically relevant prostate cancer therapies target the androgen receptor, our studies would suggest that inhibition of androgen signaling will result in reactivation of *PCAT29*, providing another mechanism underlying the effectiveness of androgen deprivation therapy.

Clinically, there is a clear need for identification of prognostic biomarkers in prostate cancer to help guide decisions on treatment intensification. The association of high *PCAT29* expression with good clinical prognosis and

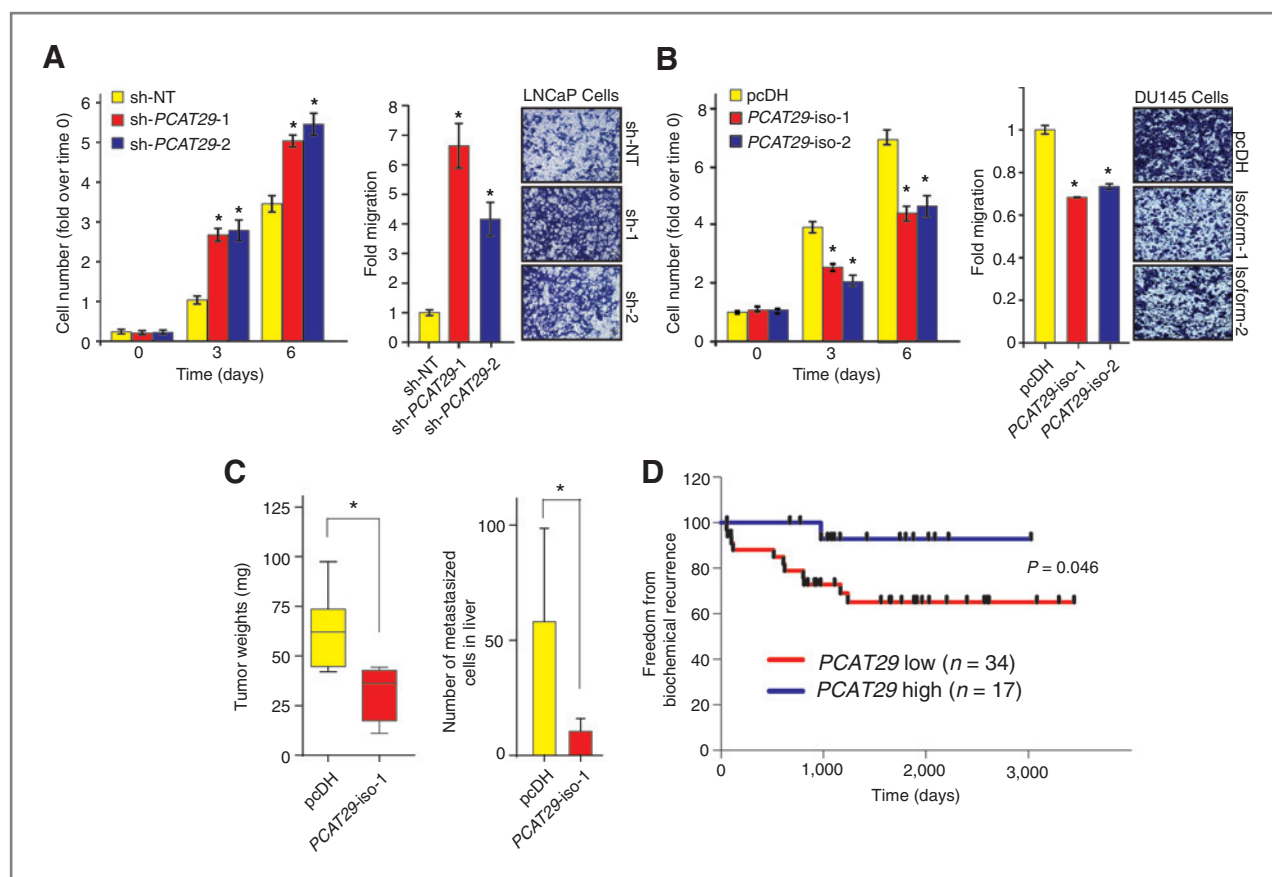


Figure 3. *PCAT29* suppresses oncogenic phenotypes. A and B, proliferation and migration of LNCaP cells stably expressing *PCAT29* shRNA (B) and DU145 cells expressing *PCAT29* expression constructs (C). Representative micrographs of crystal violet-stained migrated cells are shown as insets. C, quantification of tumor weight and metastasis to liver for 22Rv1 cells expressing *PCAT29*-isoform 1 or empty vector (pcDH) in the CAM assay. Data, mean \pm SEM. *, $P < 0.05$ by the Student *t* test. D, Kaplan–Meier analyses of prostate cancer outcomes. *PCAT29* expression was measured by qPCR and 51 patients were stratified according to their *PCAT29* expression. Patient outcomes were analyzed for freedom from biochemical recurrence.

preclinical suppression of cell proliferation and tumor metastases suggests that decreased expression or loss of *PCAT29* may identify subsets of patients who may require further intensification of therapy. As our clinical cohort was composed of hormone-sensitive disease from patients with prostatectomy, further studies need to be performed to determine whether *PCAT29* can also serve as a prognostic biomarker in the context of more advanced, castration-resistant disease. Regardless, this study highlights the importance of lncRNAs in prostate cancer biology and prognosis and suggests the need for further research in this relatively unexplored area.

Disclosure of Potential Conflicts of Interest

J.R. Prensner has ownership interest as a co-inventor on prostate cancer ncRNA patent licensed to GenomeDx Biosciences Inc., including PCATs in prostate cancer. M. Iyer has ownership interest in a patent (ncRNA and uses thereof). A.M. Chinnaiyan is a consultant/advisory board member for Wafergen Inc. No potential conflicts of interest were disclosed by the other authors.

Authors' Contributions

Conception and design: R. Malik, D.R. Robinson, F.Y. Feng, A.M. Chinnaiyan
Development of methodology: R. Malik, L. Patel, J.R. Prensner, M.K. Iyer, I.A. Asangani, X. Jing, X. Cao, A.M. Chinnaiyan

Acquisition of data (provided animals, acquired and managed patients, provided facilities, etc.): R. Malik, L. Patel, J.R. Prensner, S. Subramanian, A. Carley, A. Sahu, S. Han, M. Liu, I.A. Asangani, X. Jing, X. Cao, S.M. Dhanasekaran, D.R. Robinson, F.Y. Feng

Analysis and interpretation of data (e.g., statistical analysis, biostatistics, computational analysis): R. Malik, L. Patel, J.R. Prensner, Y. Shi, M.K. Iyer, A. Carley, Y.S. Niknafs, A. Sahu, I.A. Asangani, S.M. Dhanasekaran, D.R. Robinson, F.Y. Feng

Writing, review, and/or revision of the manuscript: R. Malik, J.R. Prensner, D.R. Robinson, F.Y. Feng, A.M. Chinnaiyan

Administrative, technical, or material support (i.e., reporting or organizing data, constructing databases): M.K. Iyer, T. Ma, X. Jing, X. Cao, D.R. Robinson, F.Y. Feng

Study supervision: R. Malik, D.R. Robinson, F.Y. Feng, A.M. Chinnaiyan

Acknowledgments

The authors thank Xia Jiang and Vishal Kothari for helpful discussions and technical assistance, as well as Karen Giles for her review of the manuscript and submission of documents. They also thank the University of Michigan Viral vector core for generating the lentiviral constructs.

Grant Support

This work was supported in part by the NIH Prostate Specialized Program of Research Excellence Grant P50CA69568, the Early Detection Research Network grant UO1 CA111275, the U.S. NIH R01CA132874-01A1, and the Department of Defense grant PC100171 (A.M. Chinnaiyan). A.M. Chinnaiyan is supported by the Doris Duke Charitable Foundation Clinical Scientist Award, the Prostate Cancer Foundation, and the Howard Hughes Medical Institute. A.M. Chinnaiyan is an American Cancer Society Research Professor and a Taubman Scholar of the

University of Michigan. F.Y. Feng was supported by the Prostate Cancer Foundation and the Department of Defense grant PC094231. R. Malik and J.R. Prensner were supported by a Prostate Cancer Foundation Young Investigator Award. R. Malik was supported by the Department of Defense Postdoctoral Fellowship W81XWH-13-1-0284. A. Sahu was supported by the NIH Predoc-

toral Fellowship 1F30CA180376-01. M. Iyer was supported by the Department of Defense Predoctoral Fellowship BC100238.

Received May 8, 2014; revised June 17, 2014; accepted June 26, 2014; published OnlineFirst July 16, 2014.

References

- Djebali S, Davis CA, Merkel A, Dobin A, Lassmann T, Mortazavi A, et al. Landscape of transcription in human cells. *Nature* 2012;489:101–8.
- Du Z, Fei T, Verhaak RG, Su Z, Zhang Y, Brown M, et al. Integrative genomic analyses reveal clinically relevant long noncoding RNAs in human cancer. *Nat Struct Mol Biol* 2013;20:908–13.
- Prensner JR, Chinnaiyan AM. The emergence of lncRNAs in cancer biology. *Cancer Discov* 2011;1:391–407.
- Guttman M, Amit I, Garber M, French C, Lin MF, Feldser D, et al. Chromatin signature reveals over a thousand highly conserved large non-coding RNAs in mammals. *Nature* 2009;458:223–7.
- Loewer S, Cabili MN, Guttman M, Loh YH, Thomas K, Park IH, et al. Large intergenic non-coding RNA-RoR modulates reprogramming of human induced pluripotent stem cells. *Nat Genet* 2010;42:1113–7.
- Tsai MC, Manor O, Wan Y, Mosammamaparast N, Wang JK, Lan F, et al. Long noncoding RNA as modular scaffold of histone modification complexes. *Science* 2010;329:689–93.
- Prensner JR, Iyer MK, Sahu A, Asangani IA, Cao Q, Patel L, et al. The long noncoding RNA SChLAP1 promotes aggressive prostate cancer and antagonizes the SWI/SNF complex. *Nat Genet* 2013;45:1392–8.
- Tomlins SA, Aubin SM, Siddiqui J, Lonigro RJ, Sefton-Miller L, Miick S, et al. Urine TMPRSS2:ERG fusion transcript stratifies prostate cancer risk in men with elevated serum PSA. *Sci Transl Med* 2011;3:94ra72.
- Lee GL, Dobi A, Srivastava S. Prostate cancer: diagnostic performance of the PCA3 urine test. *Nat Rev Urol* 2011;8:123–4.
- Asangani IA, Ateeq B, Cao Q, Dodson L, Pandhi M, Kunju LP, et al. Characterization of the EZH2-MMSET histone methyltransferase regulatory axis in cancer. *Mol Cell* 2013;49:80–93.
- van der Horst EH, Leupold JH, Schubert R, Ullrich A, Allgayer H. TaqMan-based quantification of invasive cells in the chick embryo metastasis assay. *Biotechniques* 2004;37:940–2, 4, 6.
- Kong L, Zhang Y, Ye ZQ, Liu XQ, Zhao SQ, Wei L, et al. CPC: assess the protein-coding potential of transcripts using sequence features and support vector machine. *Nucleic Acids Res* 2007;35:W345–9.
- Yu J, Mani RS, Cao Q, Brenner CJ, Cao X, Wang X, et al. An integrated network of androgen receptor, polycomb, and TMPRSS2-ERG gene fusions in prostate cancer progression. *Cancer Cell* 2010;17:443–54.
- Nie L, Wu HJ, Hsu JM, Chang SS, Labaff AM, Li CW, et al. Long non-coding RNAs: versatile master regulators of gene expression and crucial players in cancer. *Am J Transl Res* 2012;4:127–50.
- Wu L, Runkle C, Jin HJ, Yu J, Li J, Yang X, et al. CCN3/NOV gene expression in human prostate cancer is directly suppressed by the androgen receptor. *Oncogene* 2014;33:504–13.

Molecular Cancer Research

The IncRNA *PCAT29* Inhibits Oncogenic Phenotypes in Prostate Cancer

Rohit Malik, Lalit Patel, John R. Prensner, et al.

Mol Cancer Res 2014;12:1081-1087. Published OnlineFirst July 16, 2014.

Updated version Access the most recent version of this article at:
doi:[10.1158/1541-7786.MCR-14-0257](https://doi.org/10.1158/1541-7786.MCR-14-0257)

Supplementary Material Access the most recent supplemental material at:
<http://mcr.aacrjournals.org/content/suppl/2014/07/19/1541-7786.MCR-14-0257.DC1>

Visual Overview A diagrammatic summary of the major findings and biological implications:
<http://mcr.aacrjournals.org/content/12/8/1081/F1.large.jpg>

Cited articles This article cites 15 articles, 3 of which you can access for free at:
<http://mcr.aacrjournals.org/content/12/8/1081.full#ref-list-1>

Citing articles This article has been cited by 5 HighWire-hosted articles. Access the articles at:
<http://mcr.aacrjournals.org/content/12/8/1081.full#related-urls>

E-mail alerts [Sign up to receive free email-alerts](#) related to this article or journal.

Reprints and Subscriptions To order reprints of this article or to subscribe to the journal, contact the AACR Publications Department at pubs@aacr.org.

Permissions To request permission to re-use all or part of this article, use this link
<http://mcr.aacrjournals.org/content/12/8/1081>.
Click on "Request Permissions" which will take you to the Copyright Clearance Center's (CCC) Rightslink site.